



Orographic barriers, high-resolution TRMM rainfall, and relief variations along the eastern Andes

Bodo Bookhagen^{1,2} and Manfred R. Strecker³

Received 13 September 2007; revised 18 December 2007; accepted 28 December 2007; published 21 March 2008.

[1] Quantifying the degree to which tectonic and erosive processes shape landscapes is key to understanding the evolution of tectonically active mountain belts. Here we explore the interplay of these two processes along the humid, eastern flank of the South American Andes. We use high-resolution Tropical Rainfall Measurement Mission (TRMM) and SRTM data to characterize elevation, relief, and hillslope angle of peak rainfall at orographic barriers. Over a distance of more than 3500 km along the eastern flanks, we find that peak rainfall (>3.5 m/yr) occurs at a mean elevation of 1.3 ± 0.17 km, a mean relief of 0.95 ± 0.08 km, and at moderate mean hillslope angles of $18.3 \pm 1.7^\circ$. We suggest that topographic relief is the best first-order rainfall predictor and we demonstrate how relief changes along strike south of the Andean orocline alter rainfall distribution. Changes in climatic, sedimentary, and tectonic processes prevent the formation of high relief amounts at the mountain front and these areas are not characterized by pronounced rainfall peak. **Citation:** Bookhagen, B., and M. R. Strecker (2008), Orographic barriers, high-resolution TRMM rainfall, and relief variations along the eastern Andes, *Geophys. Res. Lett.*, 35, L06403, doi:10.1029/2007GL032011.

1. Introduction

[2] Catchment topography depends to a large extent on the interaction between hillslope and channel processes. Consequently, rainfall is one of the most important factors for shaping hillslope morphology and determining fluvial network characteristics in active mountain belts [e.g., Bonnet and Crave, 2003; Coppus and Imeson, 2002; Tucker and Bras, 1998]. It has been suggested that hillslope morphology is controlled by regularly exceeding thresholds for runoff erosion during large storms [e.g., Horton, 1945; Montgomery and Dietrich, 1989]. Thus, identifying the dominant elements of peak rainfall formation is key to understanding landscape dynamics and evolution [Montgomery, 2001; Roe et al., 2003]. However, rainfall distribution on windward mountain flanks is highly disparate and results from complex atmospheric-orographic interactions [e.g., Barros and Lettenmaier, 1994; Roe, 2005]. Here, we analyze variations in rainfall and topography at high resolution along the eastern flank of the Andes. We processed orbital TRMM data to achieve the highest,

instrument-native rainfall resolution. First, we quantify the general rainfall gradients and moisture flux in order to determine an empirical relation between rainfall and topographic relief that is necessary to produce a significant orographic rainfall peak. Second, we show that hillslope angles respond to rainfall variations in two end-member scenarios: In regions with rainfall amounts above the triggering threshold for many erosive processes, hillslope angles remain moderately steep, regardless of tectonic activity and differences in lithology. In contrast, hillslope angles in regions with lower rainfall amounts are more strongly controlled by the regional tectonic and sedimentation characteristics, as well as lithology. Third, moisture flux into the orogen varies roughly by a factor of two, but peak-rainfall amounts remain constant for regions with similar relief characteristics.

2. Methods and Data

[3] We processed rainfall data from the Tropical Rainfall Measurement Mission (TRMM). The TRMM platform has several sensors that help characterize the global hydrological cycle between 36°N and 36°S [e.g., Kummerow et al., 2000]. We rely on two different data products with different spatiotemporal resolution. First, the spatially high-resolution TRMM 2B31 data product and second, the temporally high, but spatially low-resolution TRMM 3B42 data product [Kummerow et al., 2000]. TRMM 2B31 is a combined rainfall-profile product from the Precipitation Radar (PR) and TRMM Microwave Imager (TMI). We processed data from 1998 to 2006, and projected them from their original resolution of 4×6 km and orbital paths to a 5×5 km grid and equal-area projection, respectively. Each of the 52011 orbits (approx. 16/day) was fitted to an equally-spaced grid with a bilinear interpolation to account for projection and resolution inhomogeneities. Prior to rainfall calibration, we scaled the TRMM 2B31 data with the number of measurements in each grid cell, because higher latitudes are more frequently measured due to the TRMM orbital paths. In order to convert the 2B31 rainfall rate into absolute rainfall, we calibrated the scaled data with gauged rainfall data from 1970 stations ranging from 10°N to 35°S [National Climatic Data Center, 2002]. 943 of these stations are located above 1 km elevation and 667 are located above 2 km elevation (see auxiliary material).¹

[4] The second data set, TRMM 3B42, is widely used, easy to process, and designed for large-scale precipitation studies. Its algorithm combines several instruments [Kummerow et al., 2000] and the output is gridded rainfall

¹Geological and Environmental Sciences, Stanford University, Stanford, California, USA.

²Now at Department of Geography, University of California, Santa Barbara, California, USA.

³Institut für Geowissenschaften, Universität Potsdam, Potsdam, Germany.

for 0.25×0.25 degree grid boxes ($\sim 30 \times 30$ km) with a 3-hour temporal resolution. In order to generate absolute rainfall amounts from 8 measurements each day, we linearly interpolated the rainfall amounts between the measurements and integrated over each day.

[5] We derived the topographic parameters from a hole-filled 90-m version of the Shuttle Radar Topography Mission (SRTM V3) [Jarvis *et al.*, 2006] and calculated the hillslope angles in degree and relief. Relief is the elevation difference between the minimum and maximum elevation in a given radius. We chose a 3-km-relief radius as this approximately represents the average hillslope length for the Andes. [Note that results do not change if we apply a larger radius.]

[6] In order to quantify the relationship between topography, relief, hillslope angles, and rainfall, we analyzed the data in a total of 115 50-km-wide and 1000-km-long swaths, perpendicular to the Andes, with a total length of 5750 km (Figure 1a). At each point in the orogen-perpendicular direction along the swath, we averaged orogen-parallel data for rainfall, elevation, and 3-km-relief (see Figure 2 for 4 examples). We chose this orientation for several reasons: (1) the moisture transport direction is controlled by the low-level Andean jet that runs along strike of the eastern Andes, (2) vertically-integrated moisture flux into each of the swaths varies only by a factor of two [here, we integrated moisture flux between the 500 m contour and the peak elevation for each swaths], (3) the Andean deformation front is roughly parallel to the trace of the subduction zone, and (4) all swaths are sub-perpendicular to major thrust faults and thus represent topographic cross sections that reflect structural characteristics of the orogen. The swaths can be viewed as 50-km-averaged topographic, hillslope, relief, and rainfall profiles. Given the 5×5 km resolution of the TRMM 2B31 data, we average data sets within a range of 5 km up- and downslope of the peak rainfall locality.

3. Moisture Transport and Rainfall Along the Eastern Flank of the Andes

[7] The Andes represent a major topographic barrier to atmospheric circulation in South America. The orogen separates sharply contrasting conditions in the humid Amazon lowlands and the generally more arid Pacific margin to the west (Figure 1b). In their central portion (15 – 27° S), the Andes form the second largest orogenic plateau, the semi-arid to arid Altiplano-Puna Plateau [e.g., Allmendinger *et al.*, 1997; Garreaud *et al.*, 2003]. The moisture source for rainfall along the eastern flank of the Andes is primarily the Atlantic Ocean with recycled moisture from the Amazon Basin [Eltahir and Bras, 1994; Vera *et al.*, 2006]. During the austral summer, a warm-core anticyclone (Bolivian High) develops in the upper troposphere over the Altiplano-Puna and the adjacent eastern Andean slopes [e.g., Garreaud *et al.*, 2003; Vera *et al.*, 2006]. Farther east is an upper-level trough extending over the western South Atlantic from where additional moisture is drawn. At low levels, a continental heat low develops in the Gran Chaco of Paraguay and Argentina and parts of the northern Sierras Pampeanas of northwest Argentina [Lenters and Cook, 1995; Vizu and Cook, 2007]. The ‘Chaco Low’ controls moisture flux into southeastern Bolivia and northwestern Argentina through the

low-level Andean jet [Salio *et al.*, 2002; Seluchi *et al.*, 2003]. Heavy orographic, convective rainfall occurs, when the moisture-laden northerly low-level flow travels along the eastern slopes of the Andes [e.g., Garreaud *et al.*, 2003; Vizu and Cook, 2007; Vuille *et al.*, 1998]. While the general atmospheric conditions leading to rainfall are fairly well known [e.g., Vera *et al.*, 2006], the topographic characteristics modulating orographic rainfall are less well known, particularly their influence on geomorphic processes. We exploit the fundamentally different relief characteristics south of the Bolivian orocline at $\sim 17^\circ$ S to characterize rainfall-controlling mechanisms.

4. Results and Discussion

[8] The new high-resolution and calibrated TRMM data reveal some striking characteristics of Andean rainfall distribution. The precise nature of the orographic rainfall patterns can only be observed in our processed TRMM 2B31 data set, whereas the coarser resolution of the TRMM 3B42 data set does not depict the peak rainfall amounts (Figure 2). Peak rainfall occurs mainly at the first topographic rise of the Andes. Two rainfall peaks exist locally, related to the eastward-directed thrusting and topographic growth of the Subandes, which has caused a moderate topographic barrier ~ 50 to 100 km (north) east of the Eastern Cordillera. In contrast to rainfall distribution along the Himalaya, however, there is no continuous inner rainfall belt as there is no pronounced two-step morphology in the Andes [Bookhagen and Burbank, 2006].

[9] Combined, all swaths reveal three principal characteristics of the rainfall-topography relations (Figure 3a). First, rainfall peaks at the eastern flanks occur at surprisingly similar elevation and relief. Second, rainfall-peak elevation is controlled by base-level conditions (or minimum elevation); third, moisture flux into the orogen varies roughly by a factor of two and moisture flux south of the orocline is comparable to regions in the northern Andes (Figure 3b). However, the fundamental difference lies in the rainfall distribution and rainfall-peak formation. For more than 3500 km length, rainfall peaks above 3.5 m/yr occur at a mean elevation of 1.3 ± 0.17 km and a 3-km-radius relief of 0.95 ± 0.08 km (or a 5-km-radius relief of 1.28 ± 0.10 km). Interestingly, all variations of rainfall-peak elevations (green line in Figure 3a) can be explained by a change in the base level (i.e., the minimum elevation defined by river system exiting the orogen) [Barros and Lettenmaier, 1994; Roe, 2005]. For example, the mean-elevation increase of ~ 0.3 km at $\sim 4^\circ$ S (3800–4000 km S-N distance along the Andes in Figure 3a) is related to the large Río Pastaza fan, which is responsible for elevated river outlets at the mountain front (black line in Figure 3a). Similarly, the Fitzcarrald arch at $\sim 11^\circ$ S (~ 3500 km) has raised the elevation of river outlets (both fan systems are depicted by light-greenish colors to the east of the Andes in Figure 1a). All rainfall peaks are associated with a critical 3-km-radius relief amount of approx. 1 km. We suggest that there is a relief threshold value at which deep convection and heavy orographic rainfall are enhanced. Hillslopes in this high-rainfall belt are covered by dense vegetation, and despite different underlying lithologies, hillslope-shaping processes have resulted in generally similar hillslope angles of $18.3 \pm 1.7^\circ$ north of the orocline.

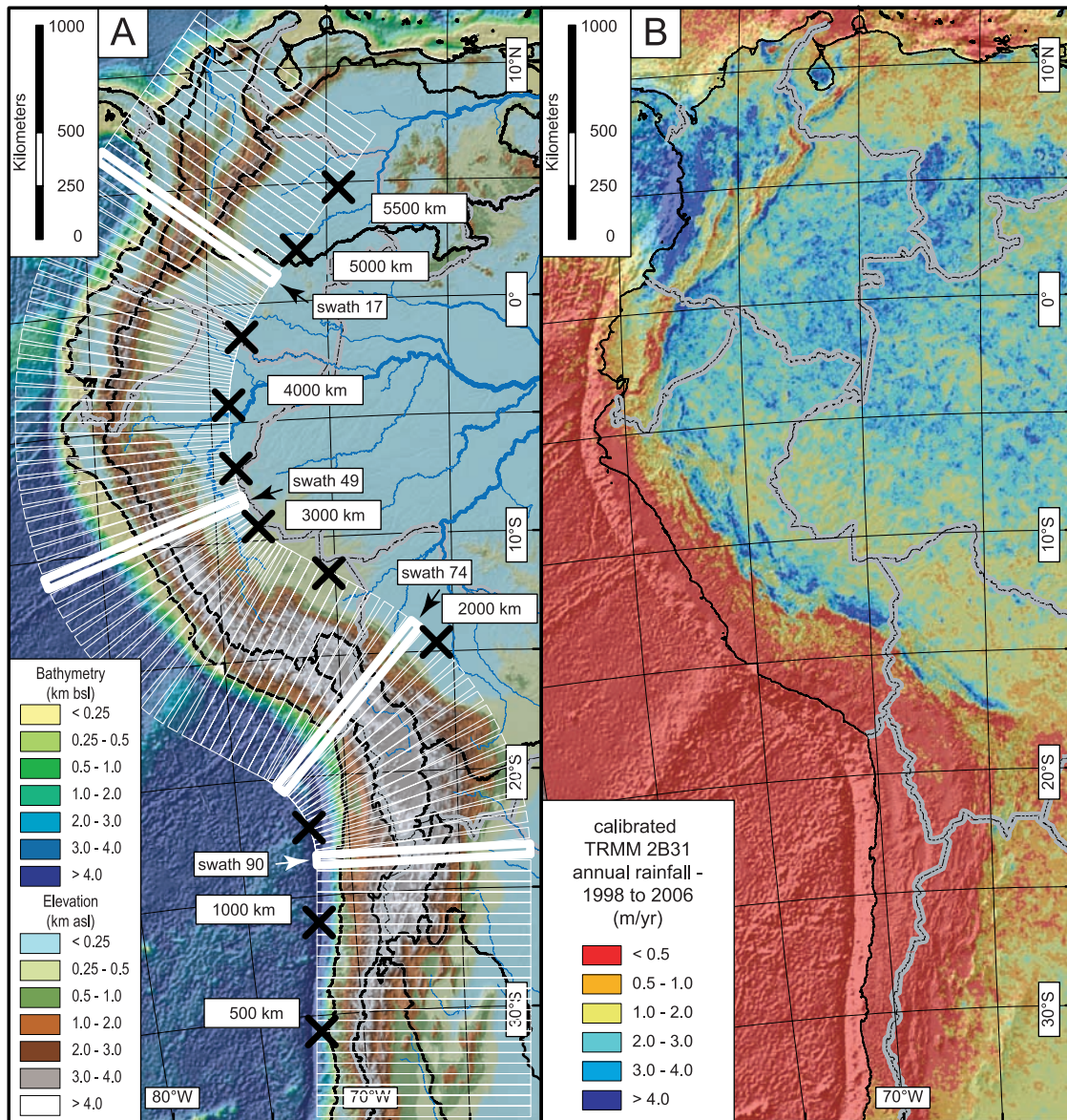


Figure 1. Color-coded topography of the Andes. White polygons mark the 115 50-km-wide and 1000-km-long swaths; bold polygons correspond to exemplary swath profiles shown in Figure 2. Swaths are oriented perpendicular to the orogen and their south to north distance along the orogen is shown by large black crosses (500-km intervals). Black lines indicate major drainage divides. Note the extensive, internally drained basin of the arid Altiplano-Puna Plateau in the orogen interior centered at $\sim 20^{\circ}\text{S}$. (b) TRMM 2B31 annual rainfall of the Andes averaged for the period of 1998 to 2006 (9 years). These data have a spatial resolution of $\sim 5 \times 5 \text{ km}^2$. Note the generally high amounts of rainfall at orographic barriers on the eastern flanks of the Andes. International borders in gray.

This suggests that the rainfall peaks with more than $\sim 3.5 \text{ m/yr}$ are above the triggering threshold for many erosive processes [Montgomery and Dietrich, 1989] and overprint any tectonic signals. However, there is a large variance in the hillslope-angle data, indicating complex interactions between various processes (e.g., groundwater sapping, landsliding, and slumping).

[10] South of the major convex eastward bend in the orogen at $\sim 17^{\circ}\text{S}$, there is no pronounced rainfall peak at the mountain front despite similar moisture flux into the orogen as in the north (Figures 3a and 3b). Peak rainfall is generally lower, but still on the order of $\sim 1.5 \text{ m/yr}$ at $\sim 26^{\circ}\text{S}$. We

explain this by a significant change in relief distribution between the northern and south-central Andes: north of the orocline, the distance from the mountain front to 1-km relief (3-km-radius) in the orogen is relatively short and less than $\sim 80 \text{ km}$. Similarly, the elevation at which relief reaches 1 km is between 1 and 1.5 km. In contrast, in the southern part of the orocline these relief contrasts are attained at much higher elevation and at much greater distance from the undeformed foreland (Figure 3b). The general relief reduction (red arrow in Figure 3a) at the mountain front in a southern direction is related to two processes. First, immediately south of $\sim 17^{\circ}\text{S}$ several megafan systems increase

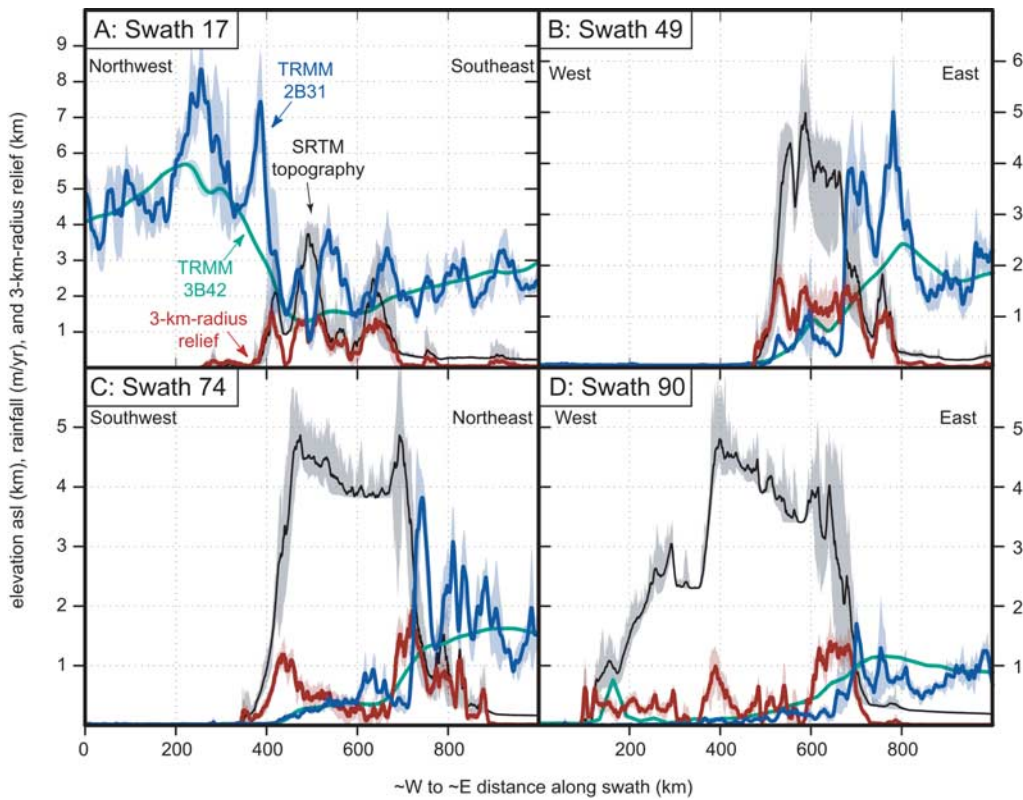


Figure 2. Four sample swath profiles from (north)east to (south)west of the northern, central, and south-central Andes (see Figure 1a for locations). Rainfall is in blue (TRMM 2B31) and green (TRMM 3B42); SRTM topography is in black and gray; and 3-km-radius relief is in red. Bold lines indicate mean values, and shading denotes $\pm 2\sigma$ ranges for the 50-km-wide and 1000-km-long swaths (note: shading for topography denotes min. and max. elevation values). (a) We observe strong orographic control of rainfall on the eastern and western side of the northern Andes, as moisture is transported from both directions. (b)–(d) Prevailing winds are from the east or northeast (right). While there is general agreement between both TRMM data sets, only the processed and calibrated TRMM 2B31 resolution is sufficient to document the strong orographic effects.

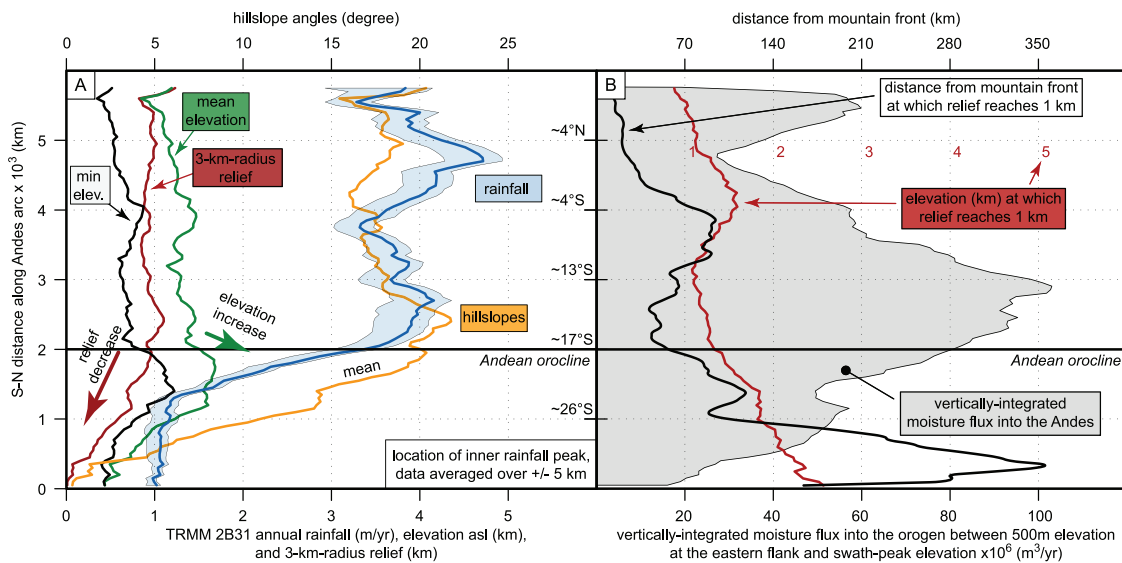


Figure 3. Synopsis of peak-rainfall analyses along 115 swath profiles. (a) We determine the peak rainfall amount (blue) and find the corresponding morphologic characteristics for each swath: mean elevation (green), minimum elevation (black), 3-km-radius relief (red), and hillslope angle (orange). For a distance of more than ~ 3500 km between 2000 and 5750 km along the eastern Andes flank, elevation (1.3 ± 0.17 km), relief (0.95 ± 0.08 km), and hillslope angles ($18.3 \pm 1.7^\circ$) at peak rainfall locations remain nearly constant. (b) South of the orocline at $\sim 17^\circ$ S, peak rainfall amounts decrease abruptly due to the combination of reduced moisture supply and <1 km relief at the mountain front.

the elevation at which the rivers exit the mountain range (green arrow in Figure 3a). The megafan systems are thought to have formed in response to a monsoonal climate in the region of the Subandes [e.g., *Horton and DeCelles*, 2001; *Leier et al.*, 2005] and probably have been in existence for the last 8 Ma [*Uba et al.*, 2007]. We do not observe megafan systems in the northern parts, as the seasonal, but almost constantly high rainfall results in continuous, efficient sediment transport away from the mountain front and thus may prevent fan formation. Second, at the southern tip of the megafan systems around 24°S in NW Argentina, relief reduction is associated with enhanced sediment storage in intermontane basins that are part of a broad zone of low-elevation ranges and intervening basins that define the Andean mountain front; in contrast to the eastern flank of the orogen, this region is also associated with a change in tectonic deformation style related to the Tertiary compressional reactivation of a Cretaceous rift province [*Grier et al.*, 1991]. Farther west and southwest in the Eastern Cordillera and the transition to the northern Sierras Pampeanas basement uplifts [e.g., *Jordan et al.*, 1983], intermontane basins were filled during Plio-Pleistocene time [*Strecker et al.*, 2007]. Often, west-vergent thrust faults produce gently windward dipping, long slopes that lack the pronounced relief contrast between foreland and mountain front of northern regions.

[11] The changes in hillslope angles mimic this pattern of tectonic-climatic interaction on rainfall distribution in the eastern central Andes: At the intersection between megafans and mountain fronts, hillslope angles are still low to moderately steep due to east-vergent thrusts [e.g., *Horton and DeCelles*, 2001]. Although exceptions exist, farther south in NW Argentina, hillslope angles are consistently low. There, the low relief of partly and fully filled intermontane basins with peak rainfall amounts of only ~1 m/yr are below the triggering threshold for efficient erosive processes. Interestingly, all patchy areas of elevated rainfall of ~3 m/yr in the Argentine Andes can be related to relief amounts of 1 km or more. For example, near Tucumán at ~27°S, relief exceeds 1 km at the mountain front and results in ~3 m/yr peak rainfall. Furthermore, our findings are comparable to observations in the Himalaya, where the frontal rainfall peak is at a 5-km-relief of 1.2 ± 0.3 km (corresponding to a 3-km-relief of ~1 km) [*Bookhagen and Burbank*, 2006]. The inner rainfall band in the Himalaya occurs only in those regions, where a similar relief amount of an additional ~1 km exists (e.g., at the southern flanks of the Greater Himalayan Crystalline province).

5. Conclusion

[12] Nearly a decade of calibrated rainfall data from the Tropical Rainfall Measurement Mission (TRMM) provide an unprecedented insight into Andean rainfall distribution at high spatial resolution. The data show strong orographic rainfall bands at significant orographic barriers. Along the eastern flanks of the Andes, our analysis of 90-m digital topography and 5-km TRMM rainfall data reveal a clear relationship between rainfall and topographic relief. Over a distance of more than 3500 km from north of the equator to the orocline at 17°S, peak rainfall occurs at a 3-km-relief of 0.95 ± 0.08 km with similar relief distribution. To the extent

that erosion is coupled to rainfall through runoff thresholds, these rainfall peaks should modulate erosion. We suggest that relief is a first-order control on orographic rainfall generation and thereby corroborate earlier findings from TRMM analysis in the Himalaya [*Bookhagen and Burbank*, 2006]. Our simple, empirical relation suggests that at least 1 km of 3-km-radius relief is needed to produce a significant rainfall peak. This conclusion is supported by our observation in the regions south of the orocline: While moisture flux is comparable to the northern Andes, there is no clear rainfall peak at the eastern, windward topographic rise. This region constitutes southern Bolivia and northwestern Argentina, where lower relief amounts at orographic barriers prevent the formation of a pronounced rainfall peak and thus inhibit areas of increased erosion compared to the north. Instead, the distribution of relief and rainfall is controlled by sedimentary processes and tectonic conditions that significantly differ from regions north of the orocline. We suggest that mountain ranges with relief below the triggering amount for orographic rainfall result in significantly different landscapes. For example, the lack of focused erosion may allow a more diffuse pattern of deformation and uplift, leading to reduced foreland connectivity of fluvial systems, and storage of sediments in intermontane basins. Indeed, this is common of regions straddling the eastern Altiplano-Puna margin that coincide with the climatic and geomorphic transition south of the orocline. The conditions in the transition zone may thus cause the orogen to grow laterally, which ultimately results in the uplift and incorporation of moisture-shielded intermontane basins into the orogenic realm [e.g., *Masek et al.*, 1994; *Sobel et al.*, 2003; *Strecker et al.*, 2007].

[13] **Acknowledgments.** Part of the data used in this study were acquired during the Tropical Rainfall Measuring Mission (TRMM), and the original algorithms were developed by the TRMM Science Team. TRMM is an international project jointly sponsored by the Japan National Space Development Agency (NASDA) and the U.S. National Aeronautics and Space Administration (NASA) Office of Earth Sciences. The ungridded TRMM 2B31 data (Version 6) is accessible at http://disc.sci.gsfc.nasa.gov/data/datapool/TRMM_DP/. We thank two anonymous reviewers for constructive comments and the DFG (Leibniz Award to M.S.) for financial support.

References

- Allmendinger, R. W., et al. (1997), The evolution of the Altiplano-Puna plateau of the central Andes, *Annu. Rev. Earth Planet. Sci.*, 25, 139–174.
- Barros, A. P., and D. P. Lettenmaier (1994), Dynamic modeling of orographically induced precipitation, *Rev. Geophys.*, 32, 265–284.
- Bonnet, S., and A. Crave (2003), Landscape response to climate change: Insights from experimental modeling and implications for tectonic versus climatic uplift of topography, *Geology*, 31, 123–126.
- Bookhagen, B., and D. W. Burbank (2006), Topography, relief, and TRMM-derived rainfall variations along the Himalaya, *Geophys. Res. Lett.*, 33, L08405, doi:10.1029/2006GL026037.
- Coppus, R., and A. C. Imeson (2002), Extreme events controlling erosion and sediment transport in a semi-arid sub-Andean valley, *Earth Surf. Processes Landforms*, 27, 1365–1375.
- Eltahir, E. A. B., and R. L. Bras (1994), Precipitation recycling in the Amazon Basin, *Q. J. R. Meteorol. Soc.*, 120, 861–880.
- Garreaud, R., et al. (2003), The climate of the Altiplano: Observed current conditions and mechanisms of past changes, *Palaeogeogr. Palaeoclimatol. Palaeoecol.*, 194, 5–22.
- Grier, M. E., et al. (1991), Andean reactivation of the Cretaceous Salta Rift, northwestern Argentina, *J. S. Am. Earth Sci.*, 4, 351–372.
- Horton, B. K., and P. G. DeCelles (2001), Modern and ancient fluvial megafans in the foreland basin system of the central Andes, southern Bolivia: Implications for drainage network evolution in fold-thrust belts, *Basin Res.*, 13, 43–63.

- Horton, R. (1945), Erosional development of streams and their drainage basins: Hydrophysical approach to quantitative morphology, *Geol. Soc. Am. Bull.*, *56*, 230–275.
- Jarvis, A., H. I. Reuter, A. Nelson, and E. Guevara (2006), Hole-filled SRTM for the globe version 3, in *CGIAR-CSI SRTM 90m Database*, CGIAR Consortium for Spatial Inf., Colombo, Sri Lanka. (Available at <http://srtm.csi.cgiar.org>)
- Jordan, T. E., et al. (1983), Andean tectonics related to geometry of subducted Nazca plate, *Geol. Soc. Am. Bull.*, *94*, 341–361.
- Kummerow, C., et al. (2000), The status of the Tropical Rainfall Measuring Mission (TRMM) after two years in orbit, *J. Appl. Meteorol.*, *39*, 1965–1982.
- Leier, A. L., et al. (2005), Mountains, monsoons, and megafans, *Geology*, *33*, 289–292.
- Lenters, J. D., and K. H. Cook (1995), Simulation and diagnosis of the regional summertime precipitation climatology of South America, *J. Clim.*, *8*, 2988–3005.
- Masek, J. G., B. L. Isacks, T. L. Gubbels, and E. J. Fielding (1994), Erosion and tectonics at the margins of continental plateaus, *J. Geophys. Res.*, *99*, 13,941–13,956.
- Montgomery, D. R. (2001), Slope distributions, threshold hillslopes, and steady-state topography, *Am. J. Sci.*, *301*, 432–454.
- Montgomery, D. R., and W. E. Dietrich (1989), Source areas, drainage density, and channel initiation, *Water Resour. Res.*, *25*, 1907–1918.
- National Climatic Data Center (2002), Global Daily Climatology Network (GDCN), V1.0, <http://www.ncdc.noaa.gov/oa/climate/research/gdcn/gdcn.html>, Asheville, N. C.
- Roe, G. H. (2005), Orographic precipitation, *Annu. Rev. Earth Planet. Sci.*, *33*, 645–671.
- Roe, G. H., D. R. Montgomery, and B. Hallet (2003), Orographic precipitation and the relief of mountain ranges, *J. Geophys. Res.*, *108*(B6), 2315, doi:10.1029/2001JB001521.
- Salio, P., et al. (2002), Chaco low-level jet events characterization during the austral summer season, *J. Geophys. Res.*, *107*(D24), 4816, doi:10.1029/2001JD001315.
- Seluchi, M. E., et al. (2003), The northwestern Argentinean low: A study of two typical events, *Mon. Weather Rev.*, *131*, 2361–2378.
- Sobel, E. R., G. E. Hilley, and M. R. Strecker (2003), Formation of internally drained contractional basins by aridity-limited bedrock incision, *J. Geophys. Res.*, *108*(B7), 2344, doi:10.1029/2002JB001883.
- Strecker, M. R., et al. (2007), Tectonics and climate of the southern central Andes, *Annu. Rev. Earth Planet. Sci.*, *35*, 747–787.
- Tucker, G. E., and R. L. Bras (1998), Hillslope processes, drainage density, and landscape morphology, *Water Resour. Res.*, *34*, 2751–2764.
- Uba, C., et al. (2007), Increased sediment-accumulation rates and climatic forcing in the central Andes during the late Miocene, *Geology*, *35*, 979–982.
- Vera, C., et al. (2006), Toward a unified view of the American monsoon systems, *J. Clim.*, *19*, 4977–5000.
- Vizy, E. K., and K. H. Cook (2007), Relationship between Amazon and high Andes rainfall, *J. Geophys. Res.*, *112*, D07107, doi:10.1029/2006JD007980.
- Vuille, M., D. R. Hardy, C. Braun, F. Keimig, and R. S. Bradley (1998), Atmospheric circulation anomalies associated with 1996/1997 summer precipitation events on Sajama Ice Cap, Bolivia, *J. Geophys. Res.*, *103*, 11,191–11,204.

B. Bookhagen, Department of Geography, University of California, Santa Barbara, Santa Barbara, CA 93106, USA. (bodo@icess.ucsb.edu)

M. R. Strecker, Institut für Geowissenschaften, Universität Potsdam, D-14476 Potsdam, Germany. (strecker@geo.uni-potsdam.de)